Anisotropic effects in bismuth-antimony superconducting alloys

N. Ya. Minina and L. A. Kirakozova

Moscow State University

(Submitted 11 November 1991)
Zh. Eksp. Teor. Fiz. **101**, 1663–1683 (May 1992)

We investigate the resistance, weak-field Hall coefficient, and Dingle temperature of $Bi_{1-x}Sb_x$ semiconducting alloys uniaxially compressed to a 0.3% strain. The dependences of the resistance and of the Hall coefficient on the strain are determined both by the anisotropy of the carrier mobility, which comes into play when the carriers are redistributed among the band extrema in the course of compression, and by the degree of uniformity of the sample. We find that for most $Bi_{1-x}Sb_x$ in the investigated density range $0.09 < x < 0.16$ exhibit a microinhomogeneity of the "cluster" type. A strong decrease of the Dingle temperature upon compression is attributed to elimination of an intervalley scattering channel on going from a three-valley to a single-valley spectrum in the course of the strain. The aggregate of the experimental data does not point to the existence of deep impurity states in the band gaps of the investigated alloys.

INTRODUCTION

It is of particular interest to use uniaxial strains, which differ in principle from hydrostatic compression by their ability to alter the anisotropy of the crystal lattice and its symmetry, as an effective method of acting on the energy spectra of multivalley materials with strongly anisotropic dispersion, such as bismuth, antimony, and their alloys.

Earlier investigations[1–4] have shown that it is precisely the breaking of the threefold symmetry of the rhombohedral lattice of these substances, by uniaxial deformation along the binary and bisector axes $\mathbf{C}_1$ and $\mathbf{C}_2$, which leads to a strong qualitative rearrangement of the band structure. The ensuing violation of the equivalence of the L-points of momentum space in which the electron (or hole, in the case of strong doping) sections of the Fermi surface (FS) are localized, leads to a distribution of the carriers among the three L_i extrema and, in the case of sufficiently strong strains, to a complete depletion of one or two L_i pockets. The dispersion law at the L points does not change noticeably in this case all the way to strains $\approx 0.3\%$ (Refs. 1 and 3), remaining strongly anisotropic with effective masses differing by more 200 times in different directions. It is therefore obvious that in the course of spillover of the carriers from "heavy" into "light" extrema and vice versa one can expect a complicated strain dependence of the conductivity, the value of which should change by several times ten times. The elimination of the depleted extrema from the scattering processes and the transition to a single-valley spectrum may become a source of valuable information on the anisotropy of the mobilities, and also on the role and magnitude of the intervalley scattering in these materials. The most interesting object for the investigation of the influence of strong anisotropic strains on the kinetics and oscillatory properties are bismuth–antimony alloys.

The alloys $Bi_{1-x}Sb_x$ constitute a continuous series of substitutional solid solutions in which a smooth restructuring is effected from the energy spectrum of Bi into the spectrum of Sb (Fig. 1a). Up to a density $x \approx 0.35$ the carrier dispersion law in L is well described by the McClure model[5,6] of the energy spectrum of pure bismuth, with the parameters taken from Ref. 7. In the density interval $0.065 \leqslant x \leqslant 0.22$ the bismuth antimony spectra go over from the semimetal to the semiconductor state with a direct gap E_{gL} at the points L (Fig. 1a), which is the minimum gap in the spectrum at $0.09 \leqslant x \leqslant 0.16$. The relative energy-scale displacement of the L_i extrema in the superconductor $Bi_{1-x}Sb_x$ by uniaxial compression is shown in Fig. 1b (Ref. 3).

Since the energy spectrum of the alloy $Bi_{1-x}Sb_x$ $(0.09 \leqslant x \leqslant 0.16)$ is determined by the carriers in the three L valleys, the spillover of electrons (in n-type alloys) or holes (p-type) is not smoothed out by the presence of one more carrier group (holes in T for Bi or holes in H for antimony) and the anisotropic effects due to this spillover (e.g., in the conductivity) are particularly clearly pronounced. In addition, owing to the low values of the Fermi energy, the band-structure change due to the anisotropic deformation (Fig. 1b) makes it possible to "spill" all the carriers into one or two valleys and pass UV in one or two extrema through the boundary of the energy bands and the corresponding band gap E_{gL}, permitting thereby an investigation of the structure of the bottom of the band and of the energy gap, viz., the degree of blurring of the boundaries or the presence of impurity levels. Since the band structure of Bi and of $Bi_{1-x}Sb_x$ alloys under strong uniaxial compression has been investigated in detail[1–4] and the strain potentials were determined with sufficient accuracy,[8,9] it is possible to establish a one-to-one correspondence between the behavior of the electron-kinetic characteristics of the material, on the one hand, and the changes produced in the energy spectrum upon deformation.

We report here an investigation of the resistivity, Hall coefficient, and the Dingle temperature in the superconducting alloys $Bi_{1-x}Sb_x$ in a wide range of antimony density $(0.09 \leqslant x \leqslant 0.16)$ following uniaxial compression along the binary and bisector axes of the sample up to a strain $\approx 0.3\%$. The composition and homogeneity of the investigated alloys were monitored.

EXPERIMENTAL PROCEDURE

Uniaxial compression of single-crystal $Bi_{1-x}Sb_x$ specimens at helium temperatures, up to a strain $\varepsilon \approx -0.3\%$, was produced by the method described in Ref. 10. We used a calibrated tension device in which the force applied along the x axis to an elastic ring of nonmagnetic steel was transformed into uniaxial compression of the investigated speci-

 © 1992 American Institute of Physics

FIG. 1. a—Restructuring of band structure of $Bi_{1-x}Sb_x$ alloys vs the antimony density x; b—restructuring of band structure $Bi_{0.9}Sb_{0.1}$ under isotropic deformation; σ—compression force.[10]

men comprising a right-angle parallelepiped measuring $3\times0.6\times0.6$ mm^3 and rigidly secured in this ring by polymerized "Aral'dit" resin in the y direction perpendicular to the x axis.

The single-crystal alloys $Bi_{1-x}Sb_x$ ($0.09\leqslant x\leqslant0.16$) were procured from various sources: the Institute of Radio and Electronics of the Russian Academy of Sciences, The Herzen Pedagogical Institute, the Berlin Humbodt university, and the Baikov Metallurgy Institute. The composition, type of conductivity, the density $n(p)$, and the carrier mobility μ at 4.2 K, as well as the helium/room-temperature resistance ratio $\rho_{4.2}/\rho_{300}$ of the investigated alloys are listed in Table I. Several samples from each set listed in Table I were investigated. They were cut from bulky single crystals along the $\mathbf{C}_2$ or $\mathbf{C}_1$ axis, the directions of which were determined accurate to 1° from the tracks of the secondary slip planes on the (111) basal plane. The samples were predominantly n-type and had different residual-impurity contents; the strong doping with tellurium was deliberate only in the case of the $Bi_{0.9}Sb_{0.1}+10^{-4}$ Te samples (series N 1 of Table I).

The antimony density in the alloy and the strain of the sample were determined selectively for typical samples of the series by x-ray diffractometry from the change of the distances between the plane as a function of x (Ref. 11) or of the compression σ, respectively. The homogeneity of the antimony distribution in the samples was monitored with a SEMOX ARL/USA microsound quantum meter, from the change of the intensity of the x-ray bremsstrahlung of the electron beam on different sections of the sample, with a scan length 80 μm and a resolution 1 μm.[1)] The electric resistance and the Hall voltage were measured by the standard method. Studying the strain dependence of the Dingle temperature T_D we investigated the quantum oscillations of the magnetoresistivity $\rho(H)$. The strain-induced change of the FS was monitored in parallel with the investigation of the kinetic characteristics of all samples in which the carrier density was high enough to observe the Shubnikov–de Haas (SdH) effect. The Fermi surface was investigated by a standard low-frequency ($f=23$ Hz) modulation procedure.

The procedure for obtaining temperatures higher than 4.2 K in an instrument with a tension device is described in detail in Ref. 10. The temperature of the sample is maintained in this case using an inverted foamed-plastic container mounted on a long steel rod serving as the support of the stretching unit. The measurement results are reported below in a sequence that makes their discussion convenient.

DINGLE TEMPERATURE AND INTERLINE SCATTERING IN BISMUTH–ANTIMONY ALLOYS AT 4.2 K

Intervalley transitions in pure Bi are effected by acoustic phonons with energy 40 K. When the temperature is lowered their contribution to the scattering decreases exponentially, so that the ratio of the relaxation times for intervalley τ_{ev} and intravalley τ_{av} scattering at 4.2 K is $\tau_{ev}/\tau_{av}\approx100$. For scattering by neutral Sb impurities and by point defects in bismuth–antimony alloys one can expect to have $\tau_{ev}\sim\tau_{av}$ already at 4.2 K (Ref. 12), but this assumption has not been directly confirmed to date.

The Dingle temperature was investigated in compression along the bisector axis, which results according to Fig. 1b in a spillover of the carriers into a descending electron extremum L_1^e from two heretofore equivalent extrema $L_{2,3}^e$. As a result, the energy spectrum of the alloy becomes single-valley at a certain strain $\varepsilon\geqslant\varepsilon_{k1}$, so that the intervalley-scattering channel can be fully excluded.

The SdH oscillations, with frequency $F=(eh/cS)$, where S is the extremal cross section of the Fermi surface

TABLE I. Compositions and characteristics of investigated alloys.

Series, №	Alloy	$\rho_{4,2}/\rho_{300}$	$n(p)$, cm^{-3}	μ, cm^2/(V·s)
		Group I		
1	n-$Bi_{0,9}Sb_{0,1}$+ +10^{-4} ат.% Te	0,59	$2,5\cdot10^{16}$	$1,2\cdot10^{6}$
2	n-$Bi_{0,89}Sb_{0,11}$	4,7	$3,8\cdot10^{15}$	$2,0\cdot10^{6}$
3	n-$Bi_{0,91}Sb_{0,09}$	4,7	$1.5\cdot10^{15}$	$6,1\cdot10^{6}$
4	n-$Bi_{0,84}Sb_{0,16}$	4,0	$3,3\cdot10^{15}$	$2,0\cdot10^{6}$
5	p-$Bi_{0,9}Sb_{0,1}$	85	$4,1\cdot10^{14}$	$9,1\cdot10^{5}$
		Group II		
6	n-$Bi_{0,87}Sb_{0,13}$	3,1	$9,0\cdot10^{15}$	$1,2\cdot10^{6}$
7	n-$Bi_{0,89}Sb_{0,11}$	4,3	$4,5\cdot10^{15}$	$3,0\cdot10^{6}$

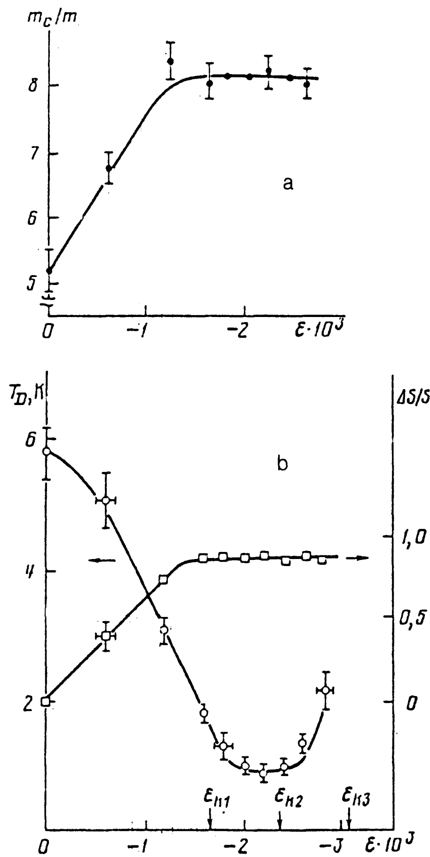

FIG. 2. a—Change of minimum cyclotron mass of sample N 1 (Table II) in compression along C_2; b—lowering of Dingle temperature (left-hand scale) and stabilization of minimum cross section of the FS "ellipsoid" L_1^e (right-hand scale) in sample No. 1 (Table II) in compression along the bisector axis.

(FS), were observed in the sample series N 1 and N 6 (Table I). The dependences of $\Delta S/S(\varepsilon)$ on the strain ε in compression along C_2 are qualitatively the same for both samples which differ only in the Sb density and in the initial carrier density. We present below data for $Bi_{0.9}Sb_{0.1}$ + 10^{-4} at. % Te with SdH oscillations of better quality. The cross sections of the FS ellipsoid corresponding to the descending extremum L_1^e increase up to a strain $\varepsilon \approx \varepsilon_{k1}$ and become stabilized after a complete carrier spillover from the $L_{2,3}^e$ extrema into L_1^e (Fig. 2a). The cross sections remain unchanged here, within a measurement accuracy (1–3)% up to the strain $\varepsilon \approx \varepsilon_{k3}$ at which overlap with the hole extrema $L_{2,3}^h$ sets in.

From the relative temperature variation of the first-harmonic oscillation amplitude

$$A \sim TH^{-1/2} \exp(-\alpha T_D/H) \sin h^{-1}(\alpha T/H),$$

where $\alpha = 0.1469(m_c/m_e)\cdot 10^3$ kOe/K and $T_D = h/(2k_B \pi \tau_D)$ τ_D is the characteristic relaxation time, k_B is the Boltzmann constant, and m_e is the free electron mass) we determined, as a function of the strain, the minimum cyclotron mass $m_c^{\min}$, whose values make it possible to calculate, from the variation of the oscillation amplitude with the magnetic field H, the corresponding variation of T_D with the strain.[13] In compression along the bisector axis, the relative change of the cyclotron mass is qualitatively analogous to the cross-section change $\Delta S/S$. The value of $m_c^{\min}$ increases by approximately 1.5 times for $\varepsilon = \varepsilon_{k1}$ and remains unchanged for $\varepsilon \geqslant \varepsilon_{k1}$ (Fig. 2b). The Dingle temperature decreases rapidly with the strain, by ≈ 6 times at $\varepsilon \approx \varepsilon_{k1}$ (Fig. 2b). This value can vary somewhat from sample to sample (see Table II).

The strong decrease of the Dingle temperature, which determines the Landau-level broadening due to scattering by impurities and to imperfection of the crystal lattice, can have two causes: 1) increase of the Fermi energy at the extremum L_1^e upon compression along the bisector axis, which decreases the effectiveness of scattering by ionized impurities; 2) elimination of an intervalley scattering channel in the transition, in the course of the deformation, from a three-valley to a single-valley spectrum.

The predominant scattering in the semiconducting $Bi_{1-x}Sb_x$ alloys at 4.2 K is from ionized impurities[14] (scattering from phonons can be neglected since as a rule $(\rho_{4.2} - \rho_{1.6})/\rho_{4.2} \approx 10^{-2}$ for these alloys). In electron scattering by a screened Coulomb potential, the scattering probability $1/\tau_\rho$ which determines the resistivity ρ is connected with $1/\tau_D$ by the relation[15]

$$\tau_D/\tau_\rho = (k-1)\left(\tfrac{1}{2}(k+1)\ln[(k+1)/(k-1)]-1\right), \qquad (1)$$

where $k = 1 + q^2/(2k_F^2)$, $1/q$ is the screening length and $k_F = [S_{\min}/(\pi\hbar^2)]^{1/2}$ is the Fermi radius; $0 < \tau_D/\tau_\rho < 1$ and τ_D/τ_ρ decreases with increase of k_F. Equation (1) takes into account the predominant contribution to the resistance from large-angle scattering. This equation holds for metals with almost spherical FS, and can be used in the case of $Bi_{1-x}Sb_x$ only to estimate limiting values. Assuming that in view of the high sensitivity of τ_D to small-angle scattering we always have $\tau_D/\tau_\rho < 1$, and that the decrease, which follows from (1), of this ratio with increase of the FS takes place also

TABLE II. Characteristics of samples of series No. 1 ($Bi_{0.9}Sb_{0.1}$ + 10^{-4} at .% Te) in investigation of the strain dependence of T_D.

№	$(m_c/m_e)10^3$		E_F, meV		T_D, K		$T_D(0)/T_D(\varepsilon_{k1})$		(τ_{iv}/τ_{av}) max	
	$\varepsilon=0$	$\varepsilon \geqslant \varepsilon_{k1}$	$\varepsilon=0$	$\varepsilon \geqslant \varepsilon_{k1}$	$\varepsilon=0$	$\varepsilon \geqslant \varepsilon_{k1}$	exp	calc	k **=0	k=0.5
1	4,0	6.0	8	15.8	5.9	0,9	6,5	3,5	1,2	0,44
2	5.3	8,2	10	16	5.8	1,0	5,8	2,7	0,9	0,43
3	5,3	8.0	7.4	12.2	8,3	2,25	3.7	2.4	1,8	0,8

*) Estimate with allowance for only scattering by an ionized impurity. **$k = (1/\tau_0)/(1/\tau_{ii})$.

in the presence of anisotropic dispersion, we obtain the inequality

$$T_D(0)/T_D(\varepsilon_{k1})=\tau_D(\varepsilon_{k1})/\tau_D(0)\leqslant\tau_p(\varepsilon_{k1})/\tau_p(0), \qquad (2)$$

where the strain interval from zero to ε_{k1} corresponds to an increase, on the average, of the Fermi energy in L_1^e from 9 to 16 meV for the three investigated samples (see Table II). If for $\varepsilon = 0$ there is only intravalley scattering, which is determined in $Bi_{1-x}Sb_x$ alloys at 4.2 K, according to Ref. 14, by the predominant scattering from ionized impurities (II) ($1/\tau_p \approx 1/r_{ii}$), then, taking into account the known energy dependence

$$\tau_{ii}\sim[m^*(E_F)]^{1/2}E_F^{3/2}\Phi(E_F), \qquad (3)$$

where $\Phi(E_F)$ is a slowly varying function, we have $\tau_p(\varepsilon_{k1})/\tau_p(0) = 3.5$ at the point of total spillover of the carriers into the extremum L_1^e. This is an upper-bound estimate, since the introduction of energy-independent scattering processes ($1/\tau_p = 1/\tau_{ii} + 1/\tau_0$) only decreases the ratio $\tau_p(\varepsilon_{k1})/\tau_p(0)$. Taking the inequality (2) into account, we can state that the experimentally observed decrease of the Dingle energy (by ≈ 6 times) cannot be attributed only to an increase of the electron energy following carrier spillover into one valley.

For agreement with experiment, it remains to assume that at $\varepsilon = 0$ there exists an intervalley scattering channel which vanishes on going from a three-valley to single-valley spectrum in the course of the deformation. In this case, at zero strain we have $1/\tau_p = 1/\tau_{ev} + 1/\tau_{av}$, where $1/\tau_{av} \approx 1/\tau_{ii} + 1/\tau_0$. At the most probable ratio of $1/\tau_{ii}$ and $1/\tau_0$ located in the interval $0 \leqslant 1/\tau_0 \leqslant 0.5 \cdot 1/\tau_{ii}$ (Ref. 16), the ratio of the intervalley and intravalley relaxation times at $\varepsilon = 0$ for sample No. 1 (Table II) does not exceed a value in the interval $0.44 \leqslant \tau_{ev}/\tau_{av} \leqslant 1.2$. Similar estimates for all the investigated samples are listed in Table II. Note that the observed increase of T_D at $\varepsilon > \varepsilon_{k2}$ (Fig. 2) is due to the appearance of intervalley transitions in the hole extrema $L_{2,3}^h$ which rise under the influence of the strain. The energy spectra of the electrons and holes in L are mirror images, as manifested by the symmetry of $T_D(\varepsilon)$ about the midpoint of the band gap ($\varepsilon \approx \varepsilon_{k2}$).

To our knowledge, the estimate obtained is the first direct evidence favoring a significant role of intervalley transitions in $Bi_{1-x}Sb_x$ alloys at 4.2 K, transitions that must be taken into account in the calculation of the kinetic characteristics of these alloys.

RESISTIVITY, HALL COEFFICIENT, AND HOMOGENEITY OF BISMUTH-ANTIMONY ALLOYS

To establish the general laws governing the kinetic characteristics of semiconducting bismuth-antimony alloys under strong compression (up to $\varepsilon \approx 0.3\%$) along the binary and bisector axes, we investigated the dependences of the resistivity and the Hall coefficient of several groups of $Bi_{1-x}Sb_x$ single crystals in a rather wide range of antimony density ($0.09 < x < 0.16$). Altogether we measured more than 50 single crystals from the indicated range of antimony density x. The characteristic "representatives" of all the available sets of samples, cut as a rule from a single bulk ingot, are listed in Table I.

The samples were compressed predominantly along the bisector axis $\mathbf{C}_2$, and the direction of the current $\mathbf{j}$ coincided with the compression direction ($\mathbf{j}\|\mathbf{C}_2$). The anisotropy of the resistivity of $Bi_{1-x}Sb_x$ is most strongly manifested in this orientation. The Hall coefficient was measured in weak magnetic fields up to 10 Oe. In samples with sufficient impurity density, SdH oscillations were additionally observed and made it possible to monitor the variation of the FS with the strain.

The resistivity change expected upon compression is determined by the restructuring of the energy spectrum and by the anisotropy of the mobilities. The mobility anisotropy is such that when the experiment is configured for compression with $\boldsymbol{\sigma}\|\mathbf{C}_2$, $\mathbf{j}\|\mathbf{C}_2$, the carriers spill over from the "lighter" valleys $L_{2,3}^e$ into the heavier L_1^e. The shift of the band extrema with strain is calculated with the aid of the strain potentials from Refs. 8 and 9. Such a shift is shown by way of example in Fig. 3 for a sample from series No. 1 (Table I) in compression along $\mathbf{C}_2$. The strain ε_{k1} corresponds here to the instant of total depletion of the extrema $L_{2,3}^e$ and to exit of the Fermi level (FL) into the band gap, while ε_{k2} corresponds to location of the Fermi level at the center of the band gap at the points $L_{2,3}$, and ε_{k3} corresponds to the FL reaching in the electron extremum L_1^e the ceiling of the valence band in $L_{2,3}^h$.

With respect to the variation of the resistivity as a function of strain $\rho(\varepsilon)$ in the indicated experimental configuration, all the investigated samples (see Table I) can be divided into two groups. Group I includes alloys whose $\rho(\varepsilon)$ dependence has characteristic peak with a height $\rho(\varepsilon)/\rho_0 \approx 10$–$25$ independent of the initial carrier density (Figs. 4 and 5). A feature of these dependences is that the resistance increases at $\varepsilon \geqslant \varepsilon_{k1}$ against the background of a FS that does not change after complete spillover of the electrons

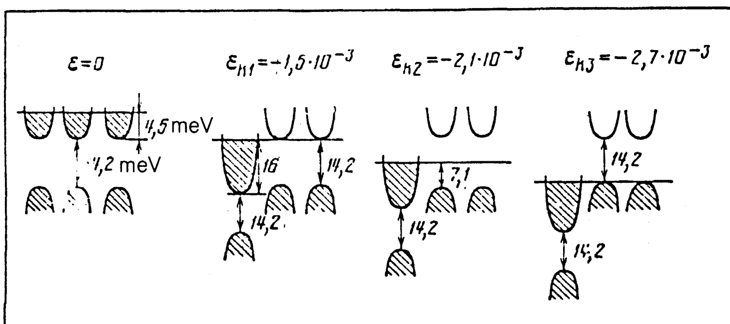

FIG. 3. Displacements of electron and hole L-extrema of samples of series No. 1 (Table I) in compression along the bisector axis.

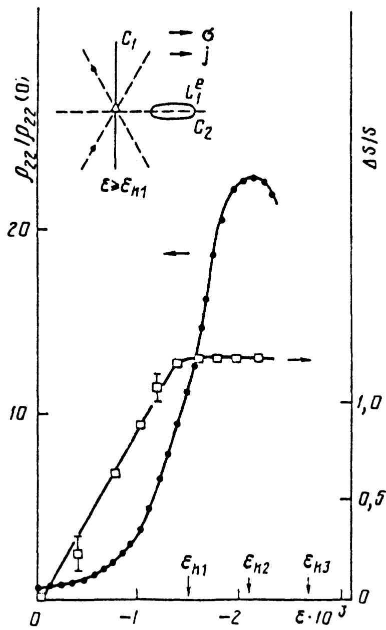

FIG. 4. Stabilization of minimum cross section of electron "ellipsoid" L_1^e (right-hand scale) and peak of resistivity (left-hand scale) for sample of series No. 1 (Table I) in compression along C_2. The inset shows the arrangement of the electron equal-energy surfaces at $\varepsilon \gg \varepsilon_{k1}$, and also the directions of the current j and of the compressing force in compression along the bisector axis.

into the extremum L_1 (Fig. 4). The dependence on the strain was peaked for the overwhelming number of investigated samples. In group II the variation of the resistivity with the strain agreed with the variation of the band structure and of the FS for only several $Bi_{1-x}Sb_x$ single crystals from the investigated density range x (series 6 and 7 of Table I). The $\rho(\varepsilon)$ plots showed first a resistivity growth by 15–30 times, followed by stabilization at $\varepsilon \gg \varepsilon_{k1}$ and a descent at $\varepsilon \approx \varepsilon_{k3}$. For the samples in which it was possible to investigate the magnetoresistance quantum oscillations, the start of

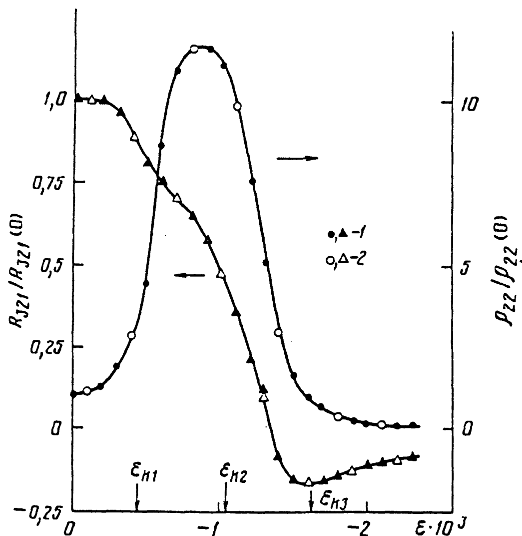

FIG. 5. Strain dependences of the relative value of the resistivity (right-hand scale) and of the Hall coefficient (left-hand scale) for sample of series No. 1 (Table I) in compression along the bisector axis: *1*—load applied, *2*—load removed.

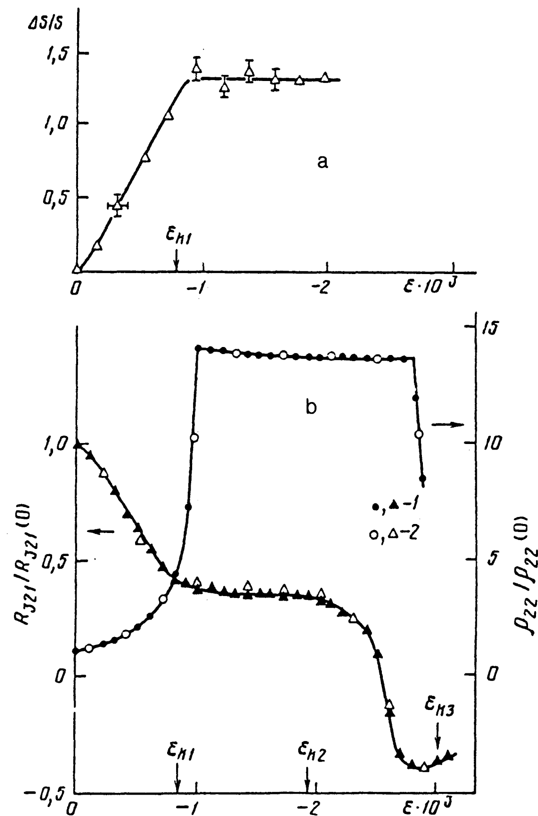

FIG. 6. a—Relative change of the cross section of the electron "ellipsoid" L_1^e of the FS of sample of series No. 6 (group II, Table I) in compression along C_2; b—strain dependence of relative resistivity (right-hand scale) and of the Hall coefficient (left-hand scale) for sample of series No. 6 (group II, Table I) in compression along the bisector axis: *1*—load applied, *2*—load removed.

the plateau on the resistivity curve correlates with saturation of the dependence of the intersection of the FS with the ellipsoid L_1^e on the uniaxial compression strain (Fig. 6).

The Hall coefficient, correspondingly, also changes qualitatively in different manners: whereas for samples with a plateau on the $\rho_{22}(\varepsilon)$ plot the strain dependence of the Hall coefficient $\rho_{321}(\varepsilon)$ also has a section where the coefficient does not vary with the strain (Fig. 6), for a sample with a resistivity peak the horizontal section is either absent or replaced by a small characteristic bend (Fig. 5). In all cases of compression along the $\mathbf{C}_2$ axis the Hall coefficient undergoes an inversion at strains $\varepsilon_{k2} < \varepsilon < \varepsilon_{k3}$.

The characteristic changes of the resistance and of the Hall coefficient in compressions $\boldsymbol{\sigma} \| \mathbf{C}_1$ and $\mathbf{j} \| \mathbf{C}_1$ are shown in Fig. 7. The resistance increases in this case by only 2–3 times, and the inversion of the Hall coefficient takes place at strains insignificantly higher than ε_{k3}.

Figures 8 and 9 show the strain dependences of the resistance at different temperatures. When the temperature is raised the peak decreases (Fig. 8) and the plateau changes into a peak whose height decreases with rise of temperature (Fig. 9). The resistance change in each loading cycle is fully reversible. The increase of the initial resistance as well as the resistance on the "plateau" of the $\rho_{22}(\varepsilon)$ curve in the temperature interval $4.2 \leqslant T \leqslant 30$ K is not caused by crystal damage, but is due to the temperature dependence; at $T > 30$ K the initial resistance of the sample shown in Fig. 9 ($E_F \sim kT$) begins to decrease.

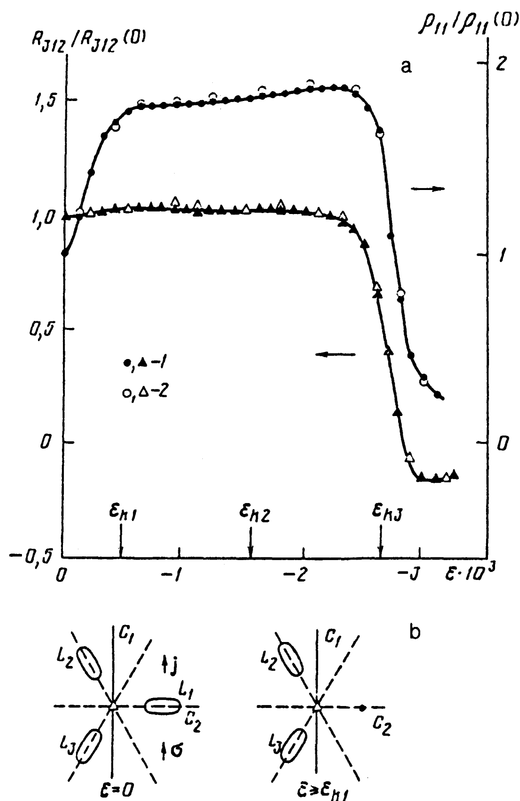

FIG. 7. a—Strain dependence of relative resistivity (right-hand scale) and Hall coefficient (left-hand scale) for sample of series No. 6 (Group II) in compression along the binary axis: *1*—load applied; *2*—load removed. b—Arrangement of band extrema at $\varepsilon = 0$ and $\varepsilon > \varepsilon_{k1}$ and also direction of current *j* and of the compression force in compression along the binary axis.

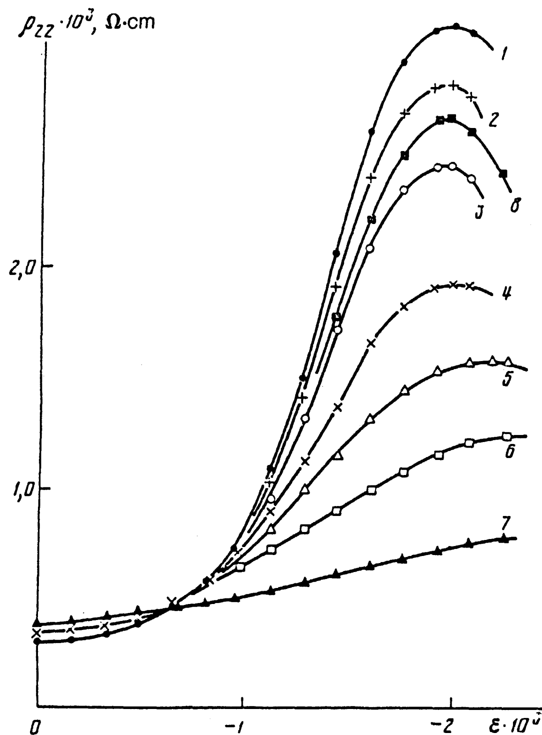

FIG. 8. Strain dependence of resistivity in compression along the C_2 axis for sample of series No. 1 (Table I) at various temperatures: *1*—4.2 K, *2*—11 K, *3*—17.5 K, *4*—26 K, *5*—32 K, *6*—41 K, *7*—58 K, *8*—14 K (last loading cycle).

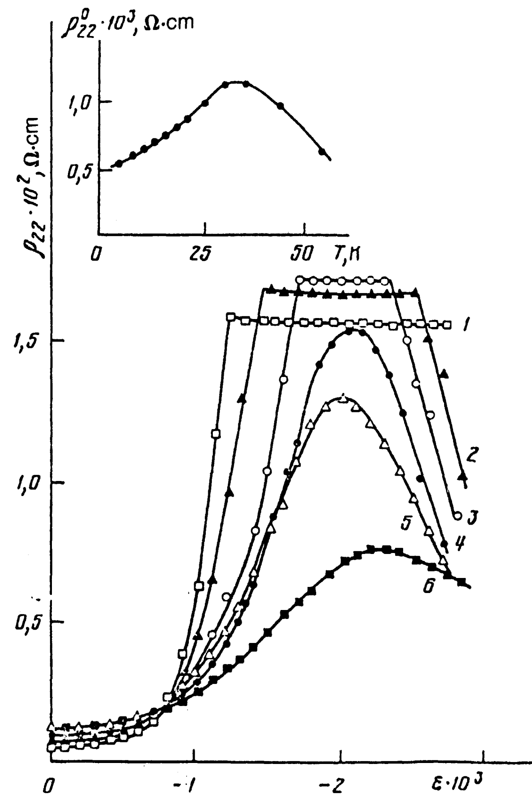

FIG. 9. Strain dependences of the resistivity in compression along the bisector axis of sample from series No. 6 (Table I) at various temperatures: *1*—4.2 K, *2*—16.7 K, *3*—20 K, *4*—25.4 K, *5*—30 K, *6*—35 K. The inset shows in enlarged scale the temperature dependence of the resistance at $\varepsilon = 0$.

Calculation of the change of the band structure by compression, similar to that shown in Fig. 3 for sample No. 1 of Table I, has established that if a sample has a resistance maximum the latter is located corresponds to the strain ε_{k2} at which the FL is in the middle of the band gap at the points $L_{2,3}$ (accurate to $\approx \pm 3$ meV). For the samples of group II, with allowance for the temperature spreading of the FL, the placement of the ends of the plateaux ε_1 and ε_3 in the strain scale, on the $\rho_{22}(\varepsilon)/\rho_{22}$ plot (Fig. 6) agree within 3 meV with the critical strain values ε_{k1} and ε_{k3} at which the FL crosses the bottom of the conduction band and the top of the valence band in $L_{2,3}$ respectively. The corresponding energy interval

$$\Delta E = \sum_{i,j=1}^{3} D_{ij}\varepsilon_{ij} = r(\varepsilon_3 - \varepsilon_1),$$

where $r = -\eta_1 D_{11} + D_{22} - \eta_3 D_{33} + \xi D_{23}$, $\eta_1 = 0.31$ and $\eta_3 = 0.42$ are the Poisson coefficients, $\xi = 0.41$ is indicative of the shear strain produced in the basal plane by compression along C_2, while D_{ij} are the strain potentials of the band gap in $L_{2,3}$ (Ref. 8). Within the accuracy limits indicated above, ΔE agrees with the band gap width E_{gL} determined from the empirical dependence on the antimony density x from Ref. 7. For example, for the samples $Bi_{0.87}Sb_{0.13}$ (No. 6, Table I) we have $\Delta E \approx 18$, whereas $E_{gL} = (10\text{–}242x)$ meV $= 21.5$ meV. The measure thermal gap for the samples of this series is ≈ 20 meV.

The cause of the strong increase of the resistivity in the

initial strain region of the investigated $Bi_{1-x}Sb_x$ samples at a compression along $\mathbf{C}_{2(1)}$ at a current $\mathbf{j}\|\mathbf{C}_{2(1)}$ is the strong anisotropy of the electron and hole valleys at the points L. Thus, according to Ref. 17, for the alloy $Bi_{0.87}Sb_{0.13}$ the ratio of the mobilities along the binary axis μ_1 and the mobility of the carriers along the bisector axis μ_2 is $\mu_1/\mu_2 = 119.6$. As a result of spillover of the carriers into the valley L_1^e with larger effective mass, the sample resistivity increases. In accordance with the form of the mobility tensor for the semiconductor $Bi_{1-x}Sb_x$ at $0 \leqslant \varepsilon \leqslant \varepsilon_{k3}$ the relative change of the resistance with the strain is determined for $0 \leqslant \varepsilon \leqslant \varepsilon_{k3}$ by the expression

$$\frac{\rho_{22}(\varepsilon)}{\rho_{22}(0)} = \frac{{}^3/_2 n_0^2 \mu_3 (\mu_1+\mu_2)}{n_0\mu_3[\mu_2 n_1(\varepsilon) + {}^1/_4(3\mu_1+\mu_2)(3n_0 - n_1(\varepsilon))] - {}^3/_4\mu_4^2 (n_1(\varepsilon)-n_0)^2}, \tag{4}$$

where n_0 is the number of electrons in each of the L extrema at $\varepsilon = 0$, n_1 is the number of electrons in L_1^e.

The spectrum of the L electrons and holes is specular in first-order approximation, and the mobilities of the holes and electrons are equal, $\mu_i^h = \mu_i^e$. Therefore for $\varepsilon \geqslant \varepsilon_{k3}$, after the electron extremum L_1^e overlaps the hole extrema $L_{2,3}^h$ we obtain

$$\frac{\rho_{22}(\varepsilon)}{\rho_{22}(0)} = \frac{{}^1/_2(1+p/N_0)(\mu_1+\mu_2)\mu_3}{\mu_3[\mu_2 + {}^1/_2 p/N_0(3\mu_1+\mu_2)] - \mu_4^2(1-p/N_0)^2}, \tag{5}$$

where p is the carrier density in one of the extrema $L_{2,3}^h$ of the valence band, and N_0 is the total electron density at $\varepsilon = 0$.

The change of the resistance upon compression along the $\mathbf{C}_2$ axis with change of the parameters of one of the samples of series No. 6 (Fig. 1, curve *1*) was calculated using expressions (4) and (5) and the dependences of the carrier densities n_1 and p on E_F at the extrema L_1^e and $L_{2,3}^h$. The initial values of the Fermi energy and of the carrier density were determined using the McClure model[6] of the energy spectrum of Bi in $Bi_{1-x}Sb_x$ alloys, with the spectrum parameters from Ref. 7. The change of the Fermi energy with strain at various L valleys were calculated using the strain potential tensor of these alloys[8,9] and the condition that the difference between the densities of the electrons and holes be preserved. We used the anisotropy of the carrier mobility in $Bi_{1-x}Sb_x$ alloys of analogous composition,[17] and the band boundaries were assumed to be distinctly demarcated.

For complete spillover of all carriers from the "lighter" valleys $L_{2,3}^e$ into the heavier valley L_1^e as a result of uniaxial compression along the $\mathbf{C}_2$ axis ($\mathbf{j}\|\mathbf{C}_2$), the relative increase of the resistance is given by

$$\frac{\rho_{22}^*}{\rho_{22}^0} = \frac{\mu_3^*(\mu_1^0+\mu_2^0)}{2(\mu_2^*\mu_3^* - \mu_4^{*2})}$$

($\mu_i^0 = \mu_i(0)$; $\mu_i^* = \mu_i(\varepsilon)$ for $\varepsilon_{k1} < \varepsilon < \varepsilon_{k3}$), which leads for the anisotropy of the mobilities from Ref. 17 to the value $\rho^*(\varepsilon)/\rho^0 = 86.7$ (for $x = 0.13$) at the instant of the total spillover of the carriers into the extremum L_1^e. This is several times larger than the experimentally observed increase $\rho_{22}(\varepsilon)/\rho_{22} \approx 15$–$30$ for samples of both groups. This discrepancy can be attributed to the fact that in the calculations no account was taken of the elimination of an intervalley scattering channel, and also of the decrease of the efficiency of scattering by an ionized impurity on account of the increase of E_F at the L_1^e extremum as the three-valley spectrum becomes single-valley as a result of the strain; this should increase, according to the data of the preceding section, the mobility μ_i^* at $\varepsilon \geqslant \varepsilon_{k1}$ by 2–4 times.

For compression along a binary axis ($\sigma\|\mathbf{C}_1$; $\mathbf{j}\|\mathbf{C}_1$), the total spillover of the carriers into two descending electron extrema L leads to a resistivity change

$$\frac{\rho_{11}^*}{\rho_{11}^0} = 2\frac{\mu_1^0+\mu_2^0}{\mu_1^*+3\mu_2^*}.$$

Since $\mu_1^0, \mu_1^* \gg \mu_2^0, \mu_2^*$, this ratio is equal to 2, in fair agreement with the experimentally observed increase of the resistance (Fig. 7). In contrast to the case of compression along $\mathbf{C}_2$, the intervalley scattering mechanism is not completely turned off here, and the Fermi energy does not increase so significantly (by $\approx 25\%$).

At first glance the inversion of the Hall coefficient in compression along the bisector axis occurs too early (Figs. 5 and 6). Actually, the contribution of the "light" holes from the $L_{2,3}^h$ extrema become decisive at strains corresponding to the energy gap between the FL in L_1^e and the ceiling of the valence band, equal to ≈ 5 meV. However, in contrast to compression along $\mathbf{C}_1$ (Fig. 7), when the mobility ratio of electrons and holes from overlapping terms $L_{2,3}^e$ and L_1^h are not so large:

$$\mu_{11}^h/\mu_{11}^e = 4\mu_1/(\mu_1+3\mu_2) \approx 4,$$

the mobility of $L_{2,3}$ holes in compression along $\mathbf{C}_2$ is higher by two orders than the mobility of the L_1 electrons

$$\mu_{22}^h/\mu_{22}^e \approx {}^3/_4\mu_1\mu_2^{-1} \approx 10^2.$$

Estimates made in the simple two-band model show that in this situation the Hall coefficient reverses sign if the density of the light holes in $L_{2,3}$ is only 0.05% of the electron density in L_1. Therefore, taking into account the temperature smearing of the FL and of the bottom of the bands, the behavior of $\rho_{321}(\varepsilon)$ at $\varepsilon \geqslant \varepsilon_{k2}$ can be fully accounted for by the appearance of thermally activated "light" holes. This conclusion is confirmed also by the fact that when the temperature is lowered the inversion point shifts into the region of large strains.

It is considerably more difficult to explain the strong decrease of the Hall coefficient at $0 \leqslant \varepsilon \leqslant \varepsilon_{k1}$ for undoped $Bi_{1-x}Sb_x$ alloys in the investigated density range upon compression along the bisector axis L according to Ref. 17, in the superconducting $Bi_{1-x}Sb_x$ at $\varepsilon = 0$ we have $\rho_{321} \approx 1/(eNc)$ and, inasmuch as for one carrier group the Hall coefficient is also equal to $1/(eNc)$, the Hall coefficient should not change on going from a three-valley to a single-valley spectrum.

Comparison with calculation (Fig. 10) gives grounds for assuming that within the framework of the existing notions concerning the band structure of $Bi_{1-x}Sb_x$ alloys and its variation under uniaxial compression, the experimental $\rho_{22}(\varepsilon)$ curves (Fig. 6), which have a clearly pronounced

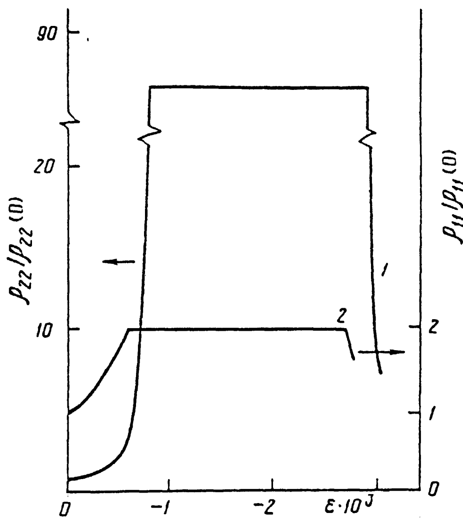

FIG. 10. Calculated plots of relative change of resistivity upon compression: *1*—along the bisector angle (left-hand scale), *2*—along the binary axis (right-hand scale). In the calculation we used the characteristics of one of the samples of series No. 6 (group II, Table I).

plateau on the segment $\varepsilon_{k1} \leqslant \varepsilon \leqslant \varepsilon_{k3}$ (at these strains the FL in the descending extremum L_1^e crosses the band gap in $L_{2,3}$—Fig. 3), reflects the spillover of the carriers and their anisotropy, and also correlates fully with the concomitant changes of the FS. On the contrary, the resistivity vs strain plots with maxima are anomalous, notwithstanding the fact that they are characteristic for the greater part of the investigated samples.

The causes of this anomalous behavior must be sought in the substantial smearing of the boundaries of the energy band, which takes place to a greater or lesser degree for all samples of group I. Leading to the same conclusion is the character of the temperature dependence of the form of the strain dependences $\rho_{22}(\varepsilon)$ (Figs. 8 and 9) which makes it possible to assume that the transformation of a plateau into a peak, which results from the temperature smearing of the energy gap, can take place also at 4.2 K as a consequence of the sufficiently strong spatial inhomogeneity of the samples. By inhomogeneity of impurity distribution we mean here microscopic fluctuations, which must be distinguished from the uniform change of the density along the length of the crystal as a result of impurity segregation in course of the growth. In the latter case one can always choose a sufficiently small section in which the density change is negligibly small.

The SEMOX ARL/USA setup used by us to monitor the homogeneity of the samples makes possible an x-ray microanalysis at a point $\sim 1\mu m^2$ and monitor continuously the ratio of the alloy components in an 80–100 μm segment. We investigated two samples from each of the two groups, with different characters of the strain dependences of the resistivity (samples No. 1, 3 of Table I with maxima and samples of type No. 6 with plateaux). Freshly cleaved (111) surfaces were scanned in 8–10 arbitrary points on the surface of each sample. Figure 11 shows characteristic spatial dependences of the x-ray intensity I corresponding to the Bi atoms (curves *1*, left-hand scale) and to Sb atoms (curves *2*, right-hand scale) for linear scanning of samples of group I (Fig. 11a, b) and samples of group II (Fig. 11c). The signals cor-

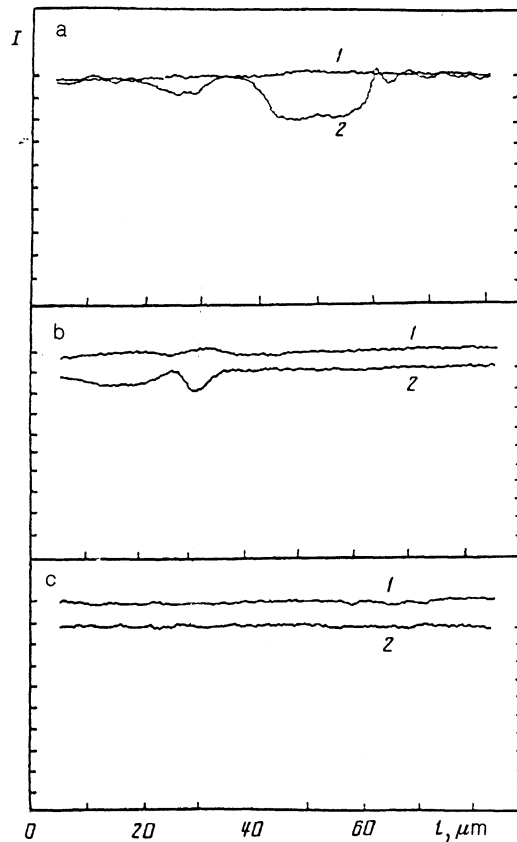

FIG. 11. Characteristic spatial dependences of the intensity of the x-rays corresponding to the Bi atoms (curves *1*, left-hand scale) and the Sb atoms (curves *2*, right-hand scale), in linear scanning: a, b—for samples of group I; c—for samples of group II.

responding to lines *1* and *2* of Fig. 11 were reckoned from the zero background ($x = 0$), and their oscillations point unambiguously to a change of the component densities in the $Bi_{1-x}Sb_x$ alloy. The signal *1* of Fig. 11 corresponds on the average to 90 at.% Bi, as against $\approx$10 at.% for signal *2*. The relatively deep minima (or maxima) on curve *2* correspond therefore to a relatively small increase (or decrease) of the intensity on curve *1*. On all, without exception, the segments of the investigated samples from group I we observed a noticeable microscopic inhomogeneity of the composition (Figs. 11a, 11b). The characteristic dimension of the regions in which the ratio of the Bi and Sb densities changes amounts to 10–30 μm, and the fluctuations of the density in them reaches 1–3 at.%. No x-ray intensity fluctuations were observed on any of the investigated scanned sections of group II (Fig. 11c).

A very clear-cut correlation exists between the character of the strain dependences of the resistivity and of the Hall coefficient, on the one hand, and the degree of homogeneity of the Sb impurity distribution in samples of groups I and II. Antimony impurity fluctuations by (1–3), at.% lead to variations of $E_{gL} = (10–242x)$ meV the bulk of the alloy by (2.5–7.5) meV, which are manifested in the kinetic effects as a smearing by the same amount. The reason is that the Fermi level in the bulk of the alloy is uniform and consequently in regions with small E_{gL} the local value of the Fermi energy is larger and complete spillover of the electrons into the L_1^e extremum occurs at larger strains, and the overlap with the

hole extremes $L^h_{2,3}$ takes place at smaller ones.

It should be noted that a temperature spreading of the gap by $2kT \approx 5$ meV ($E_{gL} \approx 20$ meV) suffices to convert the plateau on a $\rho(\varepsilon)$ plot into a peak by the action of temperature (Fig. 9). The presence of peaked strain dependences in the resistivity in $Bi_{1-x}Sb_x$ at 4.2 K is fully explained by the considered fluctuations of the densities of the alloy Bi and Sb components, leading to variation of the energy gap by up to 7.5 meV.

An additional cause of smearing the energy-band boundaries can also be the fluctuations of the charged-impurity density, especially in doped (No. 1, Table I) or compensated (No. 5, Table I) $Bi_{1-x}Sb_x$ alloys. It is impossible to observe such fluctuations in the investigate samples with the apparatus employed, since its sensitivity limit is ~ 0.5 at.%.

The foregoing data offer evidence that a characteristic feature of single-crystal $Bi_{1-x}Sb_x$ alloys is not the aforementioned specific inhomogeneity, which is determined apparently by the crystal growth conditions and amounts to the presence of microscopic regions in which the component ratio differs from that in the bulk of the sample. While the opinion that $Bi_{1-x}Sb_x$ single crystals are of high grade and have negligibly small smearing of the energy-band boundaries, based on the quantum oscillatory effects in these alloys, is valid for individual samples, is on the whole an exaggeration. The existence of oscillatory effects, just as the quite distinct diffraction peaks in the x-ray investigations, reflects only the homogeneity of the greater part of the sample volume. In the case of a strong anisotropic spectrum and anisotropic deformation, which permit the FL to be continuously passed in the course of a single experiment through the bottom of the energy band and through the band gap, the transport properties turned out to be more sensitive to inhomogeneity.

The form of the strain dependences of the resistivity and of the Hall coefficient can serve as a good criterion of the crystalline perfection of the alloy and of the sharp definition of the band boundaries. One cannot exclude the possibility that selection of samples with very distinct band boundaries can lead to a certain success in their practical utilizations as receivers (and possibly also sources) of IR radiation. The uniaxial deformation method we used to study the band structure is promising for the investigation of the impurity states of $Bi_{1-x}Sb_x$ as well as of other semiconductors with narrow band gaps.

IMPURITY LEVELS IN THE BAND GAP OF SEMICONDUCTING $Bi_{1-x}Sb_x$

Owing to the specific properties of bismuth–antimony alloys (high dielectric constant, low carrier effective mass $m^* \sim 10^{-2} m_e$) it is assumed that donor or acceptor impurities form shallow levels and distort little the band spectrum, leading only to a small tail, on the order of 1 meV, of the density of states on the band boundary.[14] The impurities are fully ionized at helium temperature.[16]

However, recent data based on investigations of the photoconductivity and of the photomagnetic effect[18] favor the existence of deep impurity states in the band gaps of semiconducting $Bi_{1-x}Sb_x$. On the basis of the temperature dependence of the Hall coefficient in the model representation that takes a deep donor level into account, the number of

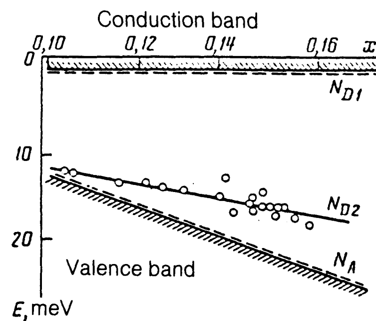

FIG. 12. Band structure of $Bi_{1-x}Sb_x$ alloys vs the antimony density x, according to the data of Ref. 18. N_A, N_{D1}—shallow acceptor and donor levels, respectively. N_{D2}—location of deep donor level as proposed in Ref. 18.

such states was estimated to be 10^{17}–10^{18} cm^{-3} (Ref. 18). The location of the level depends on the Sb density (Fig. 12).

The presence of a deep impurity level N_{D2} (in the notation of Ref. 18) should influence noticeably the kinetic and oscillatory properties of the material in the case when such a level lands in the band of alloyed states and becomes resonant.

Uniaxial compression along the bisector (binary) axis afforded a unique possibility of pass the FL at the extremum L_1 ($L_{2,3}$) through the band gap at the points $L_{2,3}$ (L_1) and to cross the N_{D2} level provided the latter did not drop substantially in the course of the deformation into the interior of the valence band. Let us analyze the degree to which the aggregate of the presented oscillatory and galvanomagnetic data offer evidence in favor of such an intersection of the FL with N_{D2}. It must be borne in mind here that the number of impurity states on the N_{D2} level reaches 10^{17}–10^{18} cm^{-3} (Ref. 18). In the investigated alloys this should lead to a steep rise of the carrier density, the initial value of which is $\approx 10^{15}$ cm^{-3}.

In the analysis of the Hall-effect data it should be noted that were the FL to pass prior to crossing the valence band through a sufficiently filled donor level located in the immediate vicinity of its ceiling, this would lead to an increase of the electron density and to further decrease of the Hall coefficient. As a result of the FL stabilization by the filled N_{D2} an increase of the carrier density in the extremum L^e_1 ($\sigma \| C_2$) or $L^e_{2,3}$ ($\sigma \| C_1$) would only initiate an overlap of the extrema L^e_1 and $L^h_{2,3}$ at $\sigma \| C_2$ or $L^e_{2,3}$ and L^h_1 at $\sigma \| C_1$, but could not lead to inversion of the Hall coefficient up to full depletion of the N_{D2} level and the onset of real overlap. The inversion would occur then at substantially larger strains than observed in experiment (Figs. 5–7).

If it is assumed, however, that the donor level near the top of the valence band does exist nonetheless, and the inversion of the Hall coefficient upon compression along the bisector axis, which takes place at $\varepsilon_{k2} < \varepsilon < \varepsilon_{k3}$ is due to the appearance of thermally activated holes, a repeated sign reversal of the Hall coefficient should be caused by the fact that the FL reached the donor level and by the strong increase of the electron density. Figure 5 shows the strain dependences of the resistance and of the Hall coefficient for n-$Bi_{0.91}Sb_{0.09}$ ($E_F \approx 2.4$ meV; sample No. 3 of Table I). It shows that at $\varepsilon \approx \varepsilon_{k3}$ the Hall coefficient is inverted and decreases smoothly with increase of the strain, which attests to

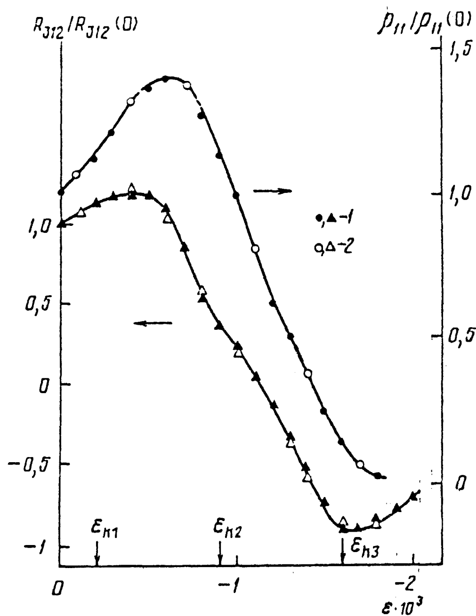

FIG. 13. Strain dependence of the relative resistivity (right-hand scale) and of the Hall coefficient (left-hand scale) for sample $p = Bi_{0.9}Sb_{0.1}$ (series No. 5, Table I) in compression along the binary axis: *1*—load applied, *2*—load removed.

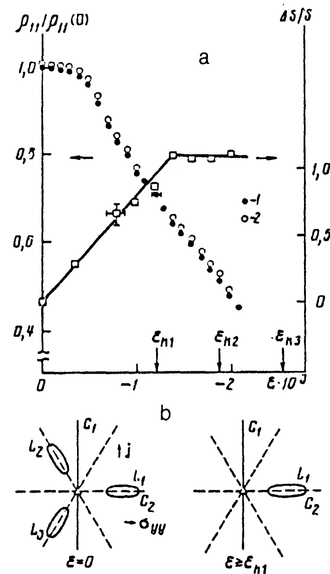

FIG. 14. a—Strain dependence of FS cross section (right-hand scale) and of resistivity (left-hand scale) for sample of series No. 1 (Table I), $\sigma \| C_2$, $j \| C_1$; b—arrangement of electron extrema in L at $\varepsilon = 0$ and $\varepsilon \gg \varepsilon_k$ and also directions of the current j and of the compression force σ.

an increase of the hole density. The strain interval in which the Hall signal due to the main contribution of the "light" holes was observed corresponds to ≈ 10 meV on the energy scale, i.e., the FL is quite deeply immersed in the valence band. A similar dependence of the weak-field Hall coefficient was observed also for compression along the binary axis (Fig. 7). These data give grounds for stating that an overlap of the electron extremum L_1^e ($L_{2,3}^e$) at $\varepsilon \approx \varepsilon_{k3}$ actually takes with the extrema $L_{2,3}^h$ (L_1^h) of the valence band.

To verify the possible rapid immersion of the N_{D2} level in the valence band in the course of deformation, we investigated compensated p-type samples (series No. 5 of Table I) in compression along the binary axis. Since the donor level N_{D2} should be empty in such samples, its lowering (with "capture" of the FL) would have led to an increase of the hole density, and a reversal of the sign of the Hall coefficient would have been observed only at $\varepsilon \gg \varepsilon_{k3}$, and furthermore under the assumption that the distance, in energy, between N_{D2} and the $L_{2,3}^e$ extrema that are lowered by the strain is shortened. The reversal of the sign of the Hall effect observed at $\varepsilon \gg \varepsilon_{k3}$ (Fig. 13) excludes the possibility of rapid descent (even at small strains) of a deep donor level into the valence band.

The invariance of the cross section $\Delta S/S$ of the Fermi surface at $\varepsilon_{k2} < \varepsilon < \varepsilon_{k3}$ (Fig. 4) confirms additionally the invariance of the carrier density in this strain interval, and offers likewise no proof that the Fermi level crosses a rather capacious donor level.

One can assume, however, that the N_{D2} level is less capacious than estimated in Ref. 18, and does not lead to a substantial change of the carrier density: a 10% increase of the carrier density corresponds to an increase of $\Delta S/S$ by only 3%, within the limits of the measurement error. Nevertheless, when landing in the band of allowed states of the extremum L_1^e, the N_{D2} level should scatter the carriers and should be manifested by a resistivity peak similar to that observed in the present study of the strain dependence of the resistivity of group-I samples. As shown above, the latter is governed by the anisotropy of the energy spectrum and by the microinhomogeneity of the $Bi_{1-x}Sb_x$ alloy. In addition, no noticeable increase of the Dingle temperature is observed on the $T_D(\varepsilon)$ dependence (Fig. 2) in the vicinity of $\varepsilon \approx \varepsilon_{k2}$, where a resistivity maximum is observed, thus confirming once more the absence of a connection between the peak and the possible resonant scattering. To shed light, nonetheless, on the question of the probability of resonant scattering, it seems necessary to investigate the $\rho_{11}(\varepsilon)$ dependences in compression along the bisector axis ($\boldsymbol{\sigma} \| \mathbf{C}_2$; $\mathbf{j} \| \mathbf{C}_1$). In this experimental configuration the descending valley L_1^e is "light" relative to the two other valleys $L_{2,3}^e$ and the assumed resonant-scattering peak should be uniquely more pronounced against the background of the resistivity that decreases with the strain. However, as shown by the data of Fig. 14, even in this case no signs of resonant scattering on passage of the FL through the band gap are observed.

Thus, the aggregate of the oscillatory and galvanomagnetic measurements of a large class of $Bi_{1-x}Sb_x$ ($0.09 \leqslant x \leqslant 0.16$) samples does not confirm the existence of a deep donor level with high impurity-state density in the band gaps of these alloys.

The experimental justification for introducing such a level in Ref. 18 was the splitting of the photoconductivity peaks of a number of $Bi_{1-x}Sb_x$ samples, but the "cluster-type" microinhomogeneity described above can cause such a splitting (if the antimony density is approximately the same in the majority of the clusters) and can thus imitate the presence of a deep impurity level. As shown above, the direct-gap fluctuation connected with the inhomogeneity of the composition amounts to 2.5–7.5 mev, which correlates with the separation of the N_{D2} level from the top of the valence band (Fig. 12), which increases with increase of the antimony content in the alloy.

In conclusion, we would like to emphasize once more

the extensive possibilities of using strong anisotropic strains to investigate the band structure of narrow-band semiconductors, and also to express our gratitude to Professor N. B. Brandt for constant interest in the work, to A. Kraapf and W. Kraak of the Humboldt University for supplying the high-grade $Bi_{1-x}Sb_x$ single crystals, and to H. Neubert and Z. Rogashevskiĭ for help with the investigation of the sample inhomogeneities.

[1)] The measurements were made at the Humboldt University in Berlin.

[1] N. B. Brandt, V. A. Kul'bachinskiĭ, N. Ya. Minina *et al.*, Zh. Eksp. Teor. Fiz. **78**, 1114 (1980) [Sov. Phys. JETP **51**, 562 (1988)].
[2] Yu. P. Gaĭdukov, N. P. Danilova, and M. B. Schchedrina-Samoilova, *ibid.* 77, 2125 (1979) [**50**, 1018 (1979)].
[3] N. B. Brandt, R. Hermann, B. A. Kul'bachinskiĭ *et al.*, Fiz. Tverd. Tela (Leningrad) **24**, 1966 (1982) [Sov. Phys. Solid State **24**, 1122 (1982)].
[4] A. L. Il'inskiĭ, O. L. Isakova, M. Y. Lavernyuk *et al.*, Vestn. MGU No. 4, 83 (1986).
[5] N. B. Brandt, R. Hermann, G. I. Bol'sheva *et al.*, Zh. Eksp. Teor. Fiz. **83**, 2152 (1982) [Sov. Phys. JETP **56**, 1247 (1982)].
[6] J. W. McClure, J. Low Temp. Phys. **25**, 57 (1976).
[7] N. B. Brandt, G. I. Golysheva, Nguen Min Thu *et al.* Fiz. Nizk. Temp. **13**, 1209 (1987) [Sov. J. Low Temp. Phys. **13**, 683 (1987)].
[8] E. V. Bogdanov, M. Yu. Lavrenyuk, and N. Ya. Minina Fiz. Tekh. Poluprov. **22**, 1348 (1988) [Sov. Phys. Semicond. **22**, 855 (1988)].
[9] M. Yu. Lavrenyuk and N. Ya. Minina, Fiz. Nizk. Temp. **14**, 52 (1988) [Sov. J. Low Temp. Phys. **14**, 27 (1988)].
[10] N. B. Brandt, V. S. Egorov, M. Yu. Lavrenyuk *et al.*, Zh. Eksp. Teor. Fiz. **89**, 2257 (1985) [Sov. Phys. JETP **62**, 1303 (1985)].
[11] H. Berger, B. Christ, and J. Troschke, Cryst. Res. and Technol. **17**, 1233 (1982).
[12] *Conduction Electrons* [in Russian], M. I. Kaganov and V. S. Edel'man, eds., Nauka (1985).
[13] L. A. Kirakozova, N. Ya. Minina, and A. M. Savin, Pis'ma Zh. Eksp. Teor. Fiz. **52**, 693 (1990) [JETP Lett. **52**, 45 (1990)].
[14] N. B. Brandt and Ya. G. Ponomarev, Zh. Eksp. Teor. Fiz. **55**, 1215 (1968) [Sov. Phys. JETP. **28**, 635 (1969)].
[15] D. Shoenberg, *Magnetic Oscillations in Metals* [Russ. transl.], Mir, 1986.
[16] N. B. Brandt, H. Littman, and Ya. G. Ponomarev, Fiz. Tverd. Tela (Leningrad) **13**, 2860 (1971) [Sov. Phys. Solid State **13**, 2408 (1971)].
[17] N. A. Rel'ko, V. I. Pol'shin, and G. A. Ivanov, Fiz. Tverd. Tela (Leningrad) **26**, 10 (1984) [Sov. Phys. Solid State **26**, 5 (1984)].
[18] V. A. Martyakhin and V. I. Trifonov, Fiz. Tekh. Poluprov. **19**, 407 (1985) [Sov. Phys. Semicond. **19**, 253 (1985)].

Translated by J. G. Adashko